

Toolkit with MATLAB GUI for Learning Position Error Signals in Data Storage Systems*

CHEE KHIANG PANG

Department of Electrical and Computer Engineering, National University of Singapore, Singapore 117576

WAI EE WONG

*Mechatronics and Recording Channel Division, Data Storage Institute, A*STAR, Singapore 117608.*

CHENGCHEN LI

Department of Electrical and Computer Engineering, National University of Singapore, Singapore 117576.

ABDULLAH AL MAMUN

Department of Electrical and Computer Engineering, National University of Singapore, Singapore 117576.

Email: eleaam@nus.edu.sg

Embedded data storage systems are becoming indispensable tools for many domestic and industrial electronic products. While Hard Disk Drives (HDDs) remain the most cost-effective form of non-volatile data storage, up and coming novel technologies such as Probe-Based Storage Systems (PBSSs) are gradually making their way into the data storage market. Unlike semiconductor memories, both HDD and PBSS use movable read/write heads for locating stored data bits. Therefore, the performance of the head positioning servomechanism of these systems plays a very important role in enhancing their storage capacities. Position Error Signal (PES), which defines the offset between the read head and the data track, is a critical element in ensuring high performance of the head positioning servomechanism and advanced methods of generating PES generation attention. This paper presents a toolkit that can be used for simulating and analyzing PES in different storage systems with movable heads. The developed toolkit with MATLAB Graphical User Interface (GUI) can be used by students to enable them to understand and visualize the PES generation process. Engineers in the data storage industry can also benefit from this toolkit in their effort to develop new, improved demodulation schemes. The developed toolkit is user-friendly and portable, with the input data and structures of different components easily changeable for rapid generation, analysis and evaluation of servo signals in PBSS and magnetic recording systems.

Keywords: position error signal; hard disk drive; probe-based storage; head positioning servo

INTRODUCTION

SINCE THE INVENTION of the internet, data storage has become one of the key elements in information technology. With the continual integration of computers and network data storage, consumers constantly demand low price, small form factor, low power consumption, and high capacity mobile storage devices. While magnetic HDDs remain as the main cost-effective source of non-volatile storage dominating the data storage market, the areal densities achievable with magnetic recording technologies will eventually reach a limit imposed by the super-paramagnetic effect. As such, many new candidates such as silicon-based semiconductor memory chips (Flash, CMOS, etc.) and Probe-Based Storage Systems (PBSS) have been proposed. The PBSS, demonstrated in the renowned 'Millipede' project

[1–3], is capable of storing huge amount of data to satisfy consumers' demands.

Fundamentally, PBSSs are based on the Scanning Probe Microscopy (SPM) and Atomic Force Microscopy (AFM) technologies developed for characterizing the surface properties in small dedicated regions. Slight modifications at the tip in the SPM system allows the surface property of the medium to be changed in nanometer scale [4]. With the bits corresponding directly to the size of the tip, PBSSs have a striking advantage in terms of areal density compared with their magnetic counterparts—the conventional and well-known HDDs.

To further increase the storage densities to meet consumer demands, more research efforts have been invested to educate undergraduate students and postgraduate students, as well as engineers working in the data storage industries, to keep up with the technological trends. With data storage systems becoming physically smaller to suit mobile consumer electronics applications, the

* Accepted 25 May 2008.

encoding methodology and signal quality of PES—the error signal between the Read/Write (R/W) element and the center of the data track—obtained are critical for fast and accurate R/W head positioning to avoid Track Mis-Registration (TMR) or 3 σ value of PES.

Ideally, the amplitude of the PES should be linearly related to the distance when the R/W element is off-track. In a typical operation, the measured PES will be channeled back into the digital servo controller in data storage systems to accurately position the mechanical actuators back into the track center for R/W operations in order to prevent destruction of user data on the adjacent tracks. As such, it is extremely crucial for students and engineers working on data storage system research to understand PES quality in accurate head positioning, especially in today's high capacity data storage systems where the tracks' proximities are squeezed into the orders of nanometers.

In this paper, the concept and usage of PES for R/W head position encoding/decoding in today's data storage systems are detailed. To assist in learning about and evaluating PES servo signal quality, a GUI written in MATLAB is developed, as GUIs are inexpensive and highly interactive tools to teach undergraduate students and graduate students in courses, as well as practicing engineers, researchers, and academics, about the operating principles of PES [5]. This methodology has been proven to be effective in aiding the educator, allowing more time for interaction between the educator and students to simulate the waveforms [6], as it is difficult to obtain or even visualize the PES from commercial HDDs. More importantly, this GUI aims to inspire the

learners to come up with novel servo encoding patterns to obtain linearity in PES for the next generation of data storage systems. The novel digital area demodulation technique developed and successfully demonstrated in [7] is employed for position decoding, and the effectiveness of the proposed GUI is verified with extensive simulation results using the PBSS.

The rest of the paper is organized as follows. First we discuss the fundamental operation principles of HDDs and PBSSs and their corresponding PES modulation schemes. Details are given of the PES generation and demodulation techniques that are used with the developed PBSS prototype, named 'Nanodrive', as an illustrative example. The components of the developed PES GUI toolkit are then explained with example simulations. Finally we give our conclusions and explore the directions for future work.

DATA STORAGE SYSTEMS

In this section, the two commonly used data storage systems employing mechanical actuators and PES (namely HDDs and PBSSs) are introduced. The similarity in their fundamental operations and usage of PES for positioning control are also highlighted.

Hard disk drives (HDD)

An HDD is a high precision and compact mechatronics device. A typical commercial HDD consists of a disk pack, actuation mechanisms and a set of R/W heads, as is shown in Fig. 1.

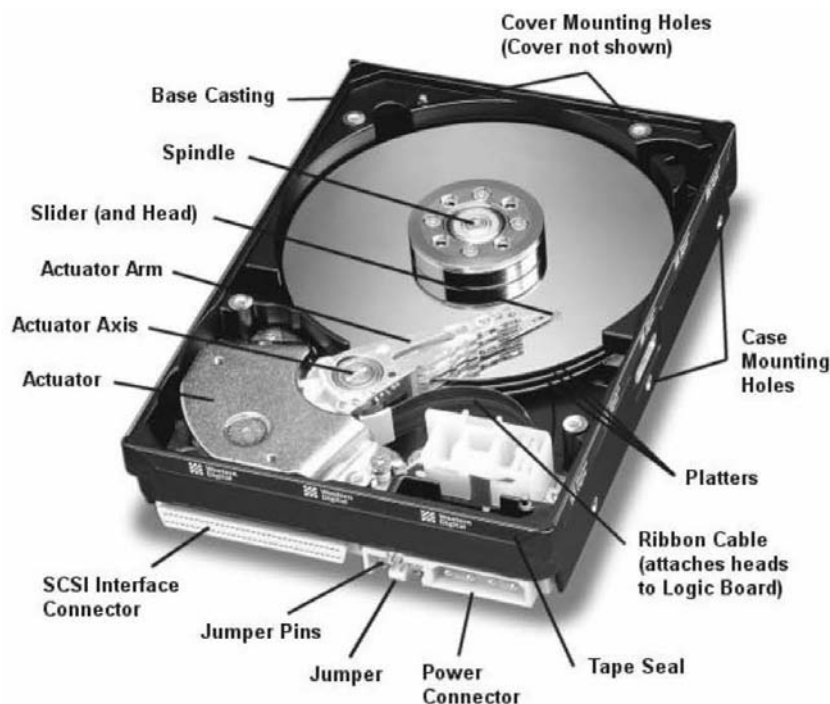


Fig. 1. Inside a typical commercial HDD.

Operation principles

The major components in a typical HDD include:

- the actuator arm driven by the VCM;
- disks that contain data and servo address information;
- the head-suspension assembly to perform R/W actions on the disks;
- the actuator assembly, which contains the VCM to drive the R/W head;
- the spindle motor assembly to cause the disks to rotate at a constant speed;
- an electronics card to serve as the interface to host computer, and
- the device enclosure, which usually contains the base plate and cover to provide support to the spindle, actuator, and electronics card, etc.

Disks are inserted into the spindle shaft (separated by spacers) and are rotated by the spindle motor at a constant revolution-per-minute (rpm). The R/W heads are mounted at the tip of the actuators protected by the sliders. Owing to the amount of air-flow generated by the high speed disk rotation, a very thin air bearing film is generated and hence the head-slider can float on the lubricant of the disks instead of being in contact with them.

Readback signal

In the magnetic HDDs, the recording channel response can be characterized by a step response, which can be derived theoretically using electromagnetic theories. A commonly used model for the readback signal is the Lorentzian function $s_{HDD}(t)$

$$s_{HDD}(t) = \frac{1}{1 + \left(\frac{2t}{PW_{50}}\right)^2} \quad (1)$$

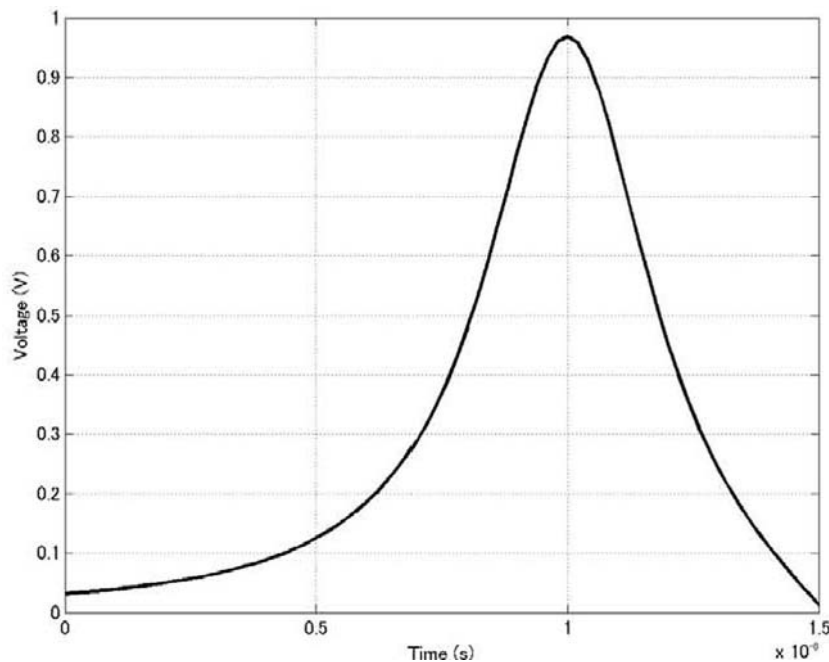


Fig. 2. Readback signal for magnetic recording technologies in HDDs.

where PW_{50} is the time duration distance between the points at which the amplitude is 50% of its peak value, and is determined by the transition width in the recording media and the R/W head-to-media distance. A picture of the simulated Lorentzian pulse when the R/W head detects a magnetic signal is shown in Fig. 2. For perpendicular magnetic recording systems, which are employed in current HDDs, an arc tangent function can be used instead to model the readback signal.

PES modulation scheme

In a typical operation, the HDD electronic circuits receive control commands from the host computer and the control signals are processed in the on-board Digital Signal Processor (DSP). On receiving the control signals, the actuator will then move and locate the R/W heads to the target locations on the disks for the R/W process to take place. During this process the PES and the track numbers are read from the disk for feedback control.

User data is recorded as magnetic domains on the disks coated with magnetic substrates in concentric circles called tracks. A typical HDD servo system consists of two types: the dedicated servo and the embedded servo (or sector servo) as shown in Fig. 3.

The earliest method of placing servo information is the dedicated servo platter, where an entire surface of one disk in the disk stack is dedicated to the servo patterns. The surface used for servo patterns are continuous around an entire revolution of the disk and so an analog and continuous time servo system can be designed, hence avoiding the sample rate and bandwidth limitations of any sampled-data system. The disadvantages of a dedi-

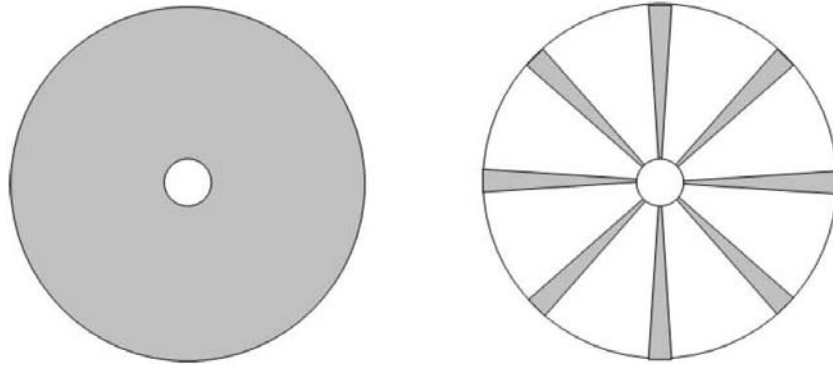


Fig. 3. The main PES encoding techniques in HDDs. Left: dedicated servo with continuous servo information on one disk surface only. Right: embedded servo with discrete sectors of servo information (in grey) on each disk.

cated servo are that it suffers from thermal off-track error, and it is not economically efficient if the number of disks in the disk stack is small. The dedicated servo uses all the tracks on one disk surface of a disk pack to store servo information, and is hence used in older generations of HDDs. In modern HDD systems, it is very hard to find a dedicated servo in actual implementations and commercially used.

Currently, most HDDs employ the embedded servo method, which divides the track into storage of user data and servo information, as most current HDDs have less disk platters. Each concentric ring on the surface on which data is recorded is referred to as a track. The position information is contained on all tracks together with the user data and other information. The servo data is recorded at regular intervals on each track, forming radial sectors as depicted by the grey regions on the right of Fig. 3. The space between the servo fields is used for data recording

and this method of implementation is referred to as embedded servo or sector servo. Sector servo can avoid the thermal track shift that is present in a dedicated servo system. Moreover, it overcomes the limitations of dedicated servos by generating the servo information with special spatial servo data patterns recorded on each of the track sectors. Embedded servos also provide the most accurate, error-free, and cost-effective head positioning technique for HDDs. Using an embedded servo, the encoded position in servo sectors can be demodulated into a track number as well as PES, which indicates the relative displacement of the head from the center of the nearest track. Interested readers are referred to [8] for in-depth discussions on different servo patterns as well as PES encoding and demodulation schemes, and [9] where multiple frequency servo bursts are used to decode PES.

Probe-based storage systems

PBSSs, on the other hand, rely on hundreds of

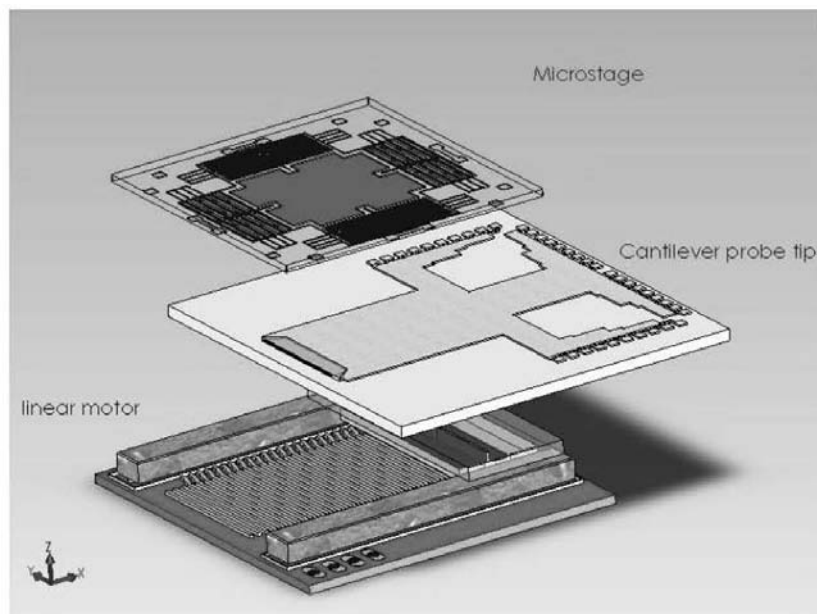


Fig. 4. Components of the 'Nanodrive' PBSS, consisting of: cantilever probe tips; a linear motor and the MEMS X-Y stage with recording medium.

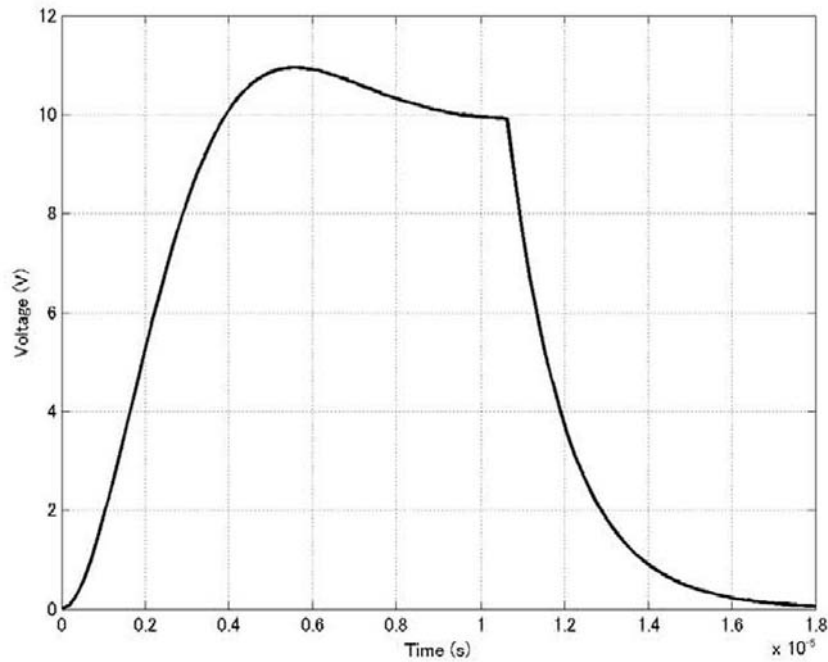


Fig. 5. Readback signal for thermomechanical pulse in PBSSs.

probes operating in parallel for high speed Read/Write/Erase (R/W/E) operations. With the successful demonstration by International business machines (IBM) in the renowned ‘Millipede’ project [1, 2, 3], many research institutes around the world are currently working on PBSSs. While their approaches may differ, the main components used for high speed parallel R/W/E of user data are similar. In the rest of this paper, the proposed so-called ‘Nanodrive’ PBSS, which was developed in the A*STAR Data Storage Institute (DSI) as shown in Fig. 4 is used.

Operation principles

The major components in a typical PBSS include:

- probes (consisting of a sharp tip on a cantilever);
- the polymer storage medium;
- a MEMS micro X-Y stage or MEMS scanner platform, and
- control, signal processing and sensor electronics, etc.

The nanometer-wide tips of the probes perform the R/W/E operations by altering the surface physics of the polymer storage medium via either (i) thermal [1, 2, 3] (ii) electric [10] or even (iii) magnetic [11] properties on a small dedicated region. The polymer storage medium is bistable and bonded on the micro X–Y stage or scanner platform during fabrication. The interference between adjacent parts must be kept to a minimum with high retention of the states after R/W/E operations to safeguard the reliability and integrity of the written-in user data. For batch fabrication, small form factor and low cost, it is desirable for

the micro X–Y stage to be fabricated using a lithography processes. The micro X–Y stage with MEMS capacitive comb driven micro-actuators should move the recording platform with a fast response, while maintaining small mechanical crosstalk (axial coupling) [12].

Readback signal

In the ‘Nanodrive’, the readback signal is obtained from thermo-mechanical properties when the heated probe tips perform R/W/E operations by altering the surface of the polymer medium, similar to that in the ‘Millipede’. As such, while the readback signal is currently not available in the ‘Nanodrive’, a transfer function for the readback signal $s_{PBSS}(s)$ is identified from the experimental data obtained in [1]

$$s_{PBSS}(s) = \frac{4.954 \times 10^{12}}{s^2 + 8.446 \times 10^5 s + 4.954 \times 10^{11}} - e^{-1.080 \times 10^{-5} s} \frac{7.039 \times 10^6}{s + 7.039 \times 10^6} \quad (2)$$

as (2) [13]. An illustration of the simulated thermo-mechanical pulse when the probe tip detects a thermo-mechanical signal is given in Fig. 5.

PES modulation scheme

Similar to HDDs, the control electronics consists of a DSP for signal processing (PES demodulation, read channel encoding/decoding and multiplexing/demultiplexing, etc.) and control signal computations. Various controllers can take charge of Input/Output (I/O) scheduling, data

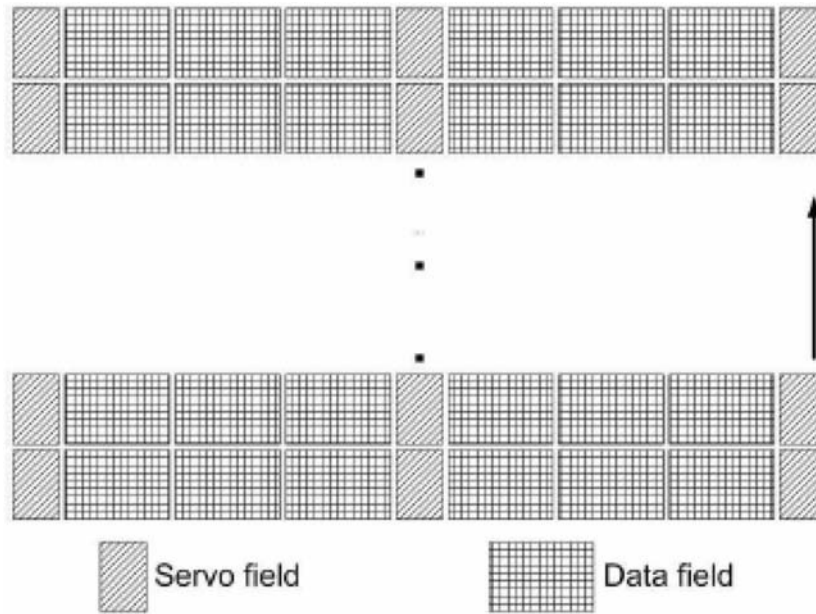


Fig. 6. Partition of PES servo field and user data field in the 'Nanodrive'.

distribution and reconstruction, host interface and failure management. A DSP works as the 'brain' of the PBSS to receive, process and output control signals in a typical operation. On receiving reference commands, the micro X-Y stage is actuated to the desired locations with the help of thermal [14] or capacitive sensors. The probes will then rely on written in PES on dedicated servo fields for R/W/E operations to take place in an array operation. The simultaneous parallel operations of large number of probes boost the data access speed tremendously.

User data is recorded as indentations on the polymer substrate in horizontal lines, also called tracks.

For the 'Nanodrive', the polymer storage medium is partitioned into five parts as can be seen in Fig. 6.

In order to control the probe tips' position more

accurately during R/W/E operations in a high density storage field, the sections at the middle and flanks of the storage medium are dedicated as servo fields where servo information is either pre-patterned on the storage medium during the fabrication process or written after system integration. These regions are not accessible for W/E operations and only the R process can take place to extract the servo bursts for PES demodulation and generation. The middle servo field is essential to ensure that the array of cantilever probe tips are at the same horizontal level at all times during R/W/E operations. The other two sections are the user data fields reserved specially for R/W/E of user data. In such a configuration, near continuous time servo system can be achieved by mimicking an embedded servo to achieve better control objectives and specifications.

From the above, it can be seen there exist many

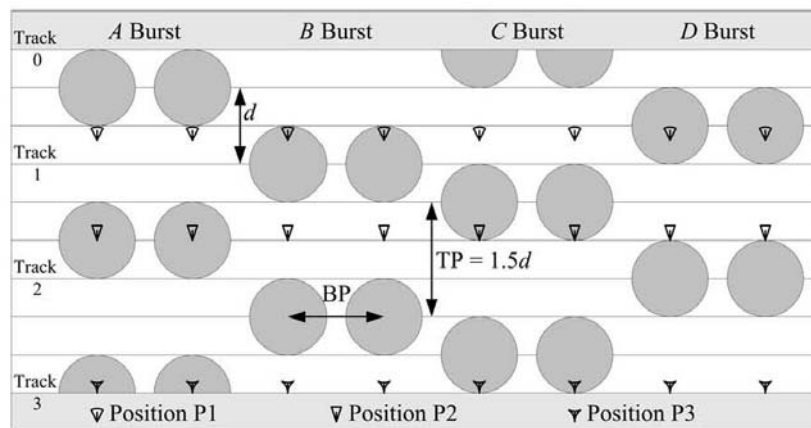


Fig. 7. Configuration of A, B, C, and D servo bursts. Only two servo bursts are displayed for each field for simplicity but without loss of generality.

inherent similarities between the two types of storage systems. The same error signal PES is used to maintain the R/W/E element on the center of the track during track following operations, in spite of the presence of external disturbances and measurement noise, which in essence is PES variance control. The track following process has to effectively reduce TMR, which is used to measure the offset between the actual head position and the track center.

PES GENERATION AND DEMODULATION

The many inherent parallelisms in data storage operations for HDDs and PBSSs have been shown. Be it HDDs or PBSSs, their servo systems use similar PES encoding/decoding methodology and identical properties, with the exception of the representation of the digital bit being either magnetic domains in HDDs or mechanical inden-

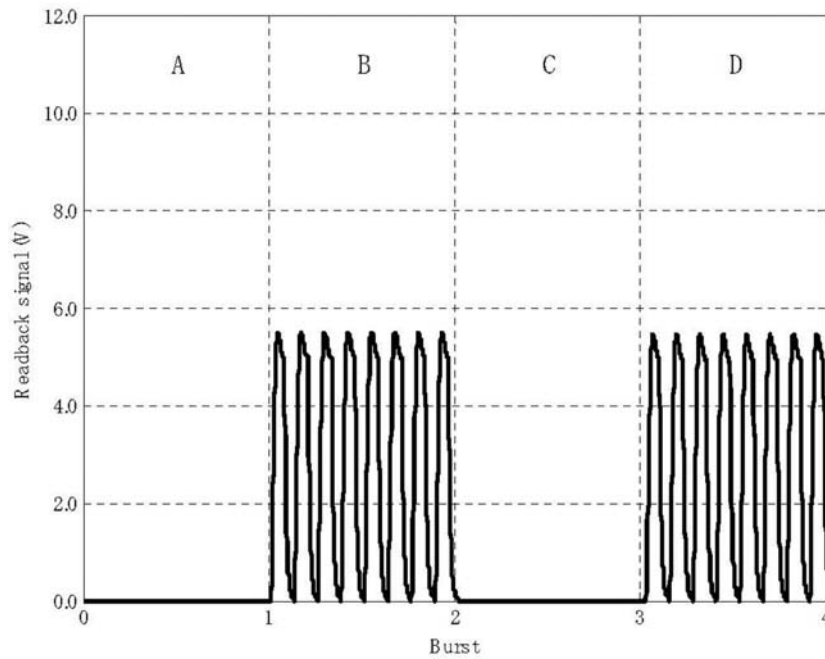


Fig. 8. Readback signal from A, B, C, and D servo bursts at $-1/6$ off Track 1 at Position P1.

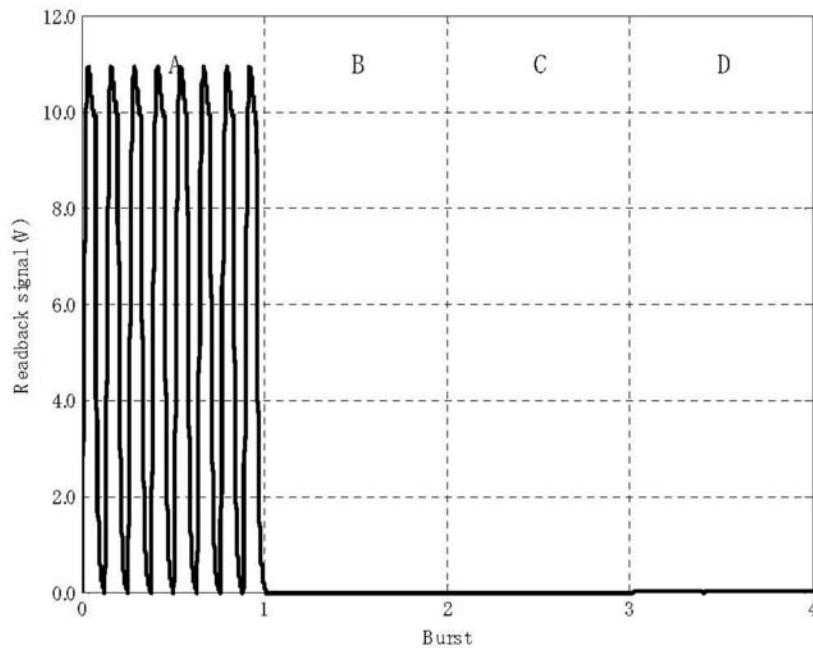


Fig. 9. Readback signal from A, B, C, and D servo bursts at $-1/2$ track offset from Track 2 at Position P2.

tations in PBSSs. In this section, the principles of PES generation and demodulation methodology will be illustrated using PBSSs as an example for simplicity but without loss of generality.

The PES signal quality and linearity are important for unique position encoding/decoding to drive the servo system for R/W/E of user data. Ideally, the magnitude of PES is a direct estimate of the vertical (cross track) distance of the tip from the track centerline, and its polarity indicates the direction of this offset. The scheme is based on the concept of mutually vertically displaced bursts analogous to magnetic recording technologies in HDDs, arranged in such a way as to provide two signals in quadrature, which can be combined to provide a robust PES. The servo marks are placed in bursts labeled *A*, *B*, *C*, and *D*, and are shown in Fig. 7.

As can be seen from Fig. 7, the centers of servo marks in *B* bursts are vertically offset from mark centers in *A* bursts by d units of length, and this amount of vertical spacing is directly related to the diameter of the written-in marks. The same principle applies to marks in quadrature bursts *C* and *D*, with the additional condition that mark centers in *C* bursts are offset by $d/2$ units from mark centers in *A* bursts in the cross-track direction. Together, the *A* and *B* bursts will be used to form the in-phase PES signal PES_p , while the *C* and *D* bursts will be used to form the quadrature-phase PES signal PES_Q , which will be detailed in the following section.

The logical marks are placed at a fixed horizontal distance from each other along a data track measured from logical mark center to logical marker center as the Bit Pitch (BP). The vertical

(cross-track) distance between neighboring tracks is known as the Track Pitch (TP), and is $1.5d$ units in length, which is different from that in magnetic recording data storage systems. It should be noted that only two logical marks are shown here for brevity but without loss of generality, although each burst typically consist of many marks to enable averaging of the corresponding readback signal.

The readback signal will be the biggest when the probe tip is at the center of the bit. It is assumed that as the probe tips move away from the center of the bit, the corresponding readback signal decreases linearly until zero when there is no logical mark under the probe tips at any arbitrary position. As such, the offset of the track center can be calculated with this readback signal relationship and is illustrated here with three typical cantilever tip positions—namely P1, P2, and P3, as shown in Fig. 7.

At Positions P1, P2, and P3, the head is on $-1/6$ track offset from the center of Track 1, at an off-track of $-1/3$ to the center of Track 2, and positioned exactly on the center of Track 3, respectively. At Position P1, the head senses no readback signal from *A* and *C* bursts because of none of logical marks are under the corresponding probe tips in that position. However, a readback signal can be obtained from *B* and *D* bursts with the same of amplitude, and is shown in Fig. 8. It is assumed that eight logical marks are used for each servo burst, although only two are shown in Fig. 7 for purposes of illustration only.

At Position P2, no readback signal can be obtained from *B*, *C*, and *D* bursts, while the probe tips sense a readback signal of full amplitude

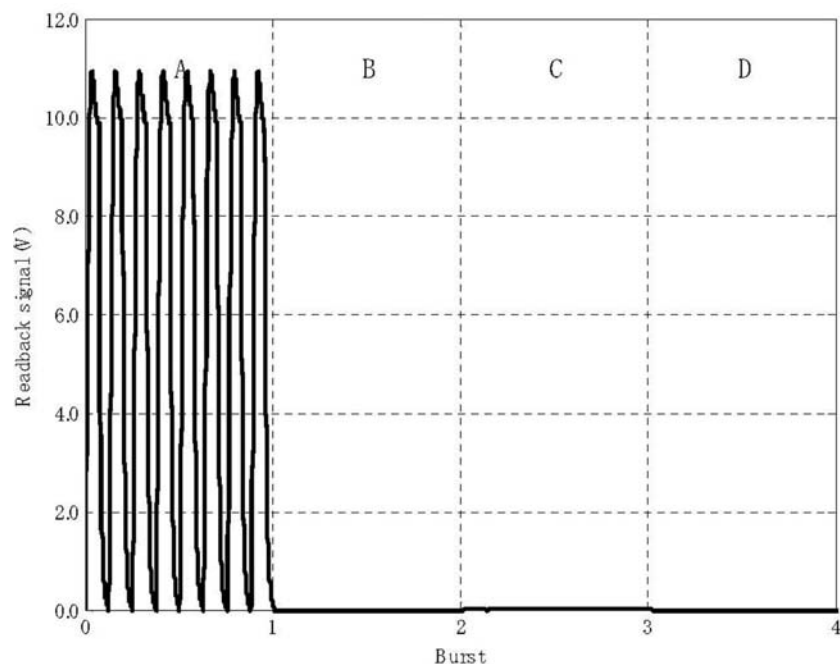


Fig. 10. Readback signal from *A*, *B*, *C*, and *D* servo bursts at center of Track 3 at Position P3.

from the A bursts. As such, the corresponding readback signal at Position P2 is obtained and is shown in Fig. 9.

At Position P3, the probe tips detect a readback signal from A bursts but not from B , C , and D bursts. Similarly, the corresponding readback signal at position P3 is shown in Fig. 10.

PES TOOLKIT SIMULATION AND DEMONSTRATION

The fundamentals and parallelisms of PES in HDDs and PBSSs having been introduced, the developed GUI in MATLAB for PES simulation and evaluation is demonstrated in this section. The PES simulation toolkit when executing the MATLAB code on initialization is shown in Fig. 11.

Features

On initialization, the default important parameters of track number and offset value are set as one and 0%, respectively, as shown in Fig. 11. In the proposed GUI toolkit environment shown in Fig. 11, the required simulation parameters (namely the R/W head offset and track number) and attribute values can easily be changed by the user, with the simulation results immediately displayed in the corresponding windows. No modification of MATLAB program source code is required as all the major and important PES related attributes are provided on the interactive GUI platform.

In top left of the GUI in Fig. 11, the readback signals of the A , B , C , and D servo bursts are displayed. When different offset values or track numbers are chosen, the amplitudes of these bursts will change and be displayed accordingly. Depend-

ing on the data storage system under study (HDDs or PBSSs), the corresponding readback signal is displayed at the bottom left of the PES simulation toolkit. In turn, the corresponding in-phase PES_P , quadrature-phase PES_Q , and combined PES are shown at the bottom right of the GUI. Since PES will be periodic in every four tracks, the GUI allows users to choose track numbers from zero to four. The range of the offset value in the slider bar is from $-1/2$ to $+1/2$ for PBSSs and -75% to $+75\%$ for magnetic recording systems. It is worth noting that the TP is 1.5 units instead of unity, which is used for our illustrations of PES encoding/decoding methodologies in PBSSs, but can easily reverted and normalized to unity in the event of evaluation of PES in magnetic recording systems.

PES generation

In this section, the PES generation technique based on digital area demodulation implemented on a PC-based spindrive servo system is used [7]. The digital area demodulation technique rectifies the digital samples of instantaneous readback signals, and the rectified samples are summed with a predetermined number of samples to fix the integration window to an integer number of periods of the burst waveform as

sum of rectified A burst sampled signal

$$= \sum_{n=1}^N |\bar{A}_n|$$

sum of rectified B burst sampled signal

$$= \sum_{n=1}^N |\bar{B}_n|$$

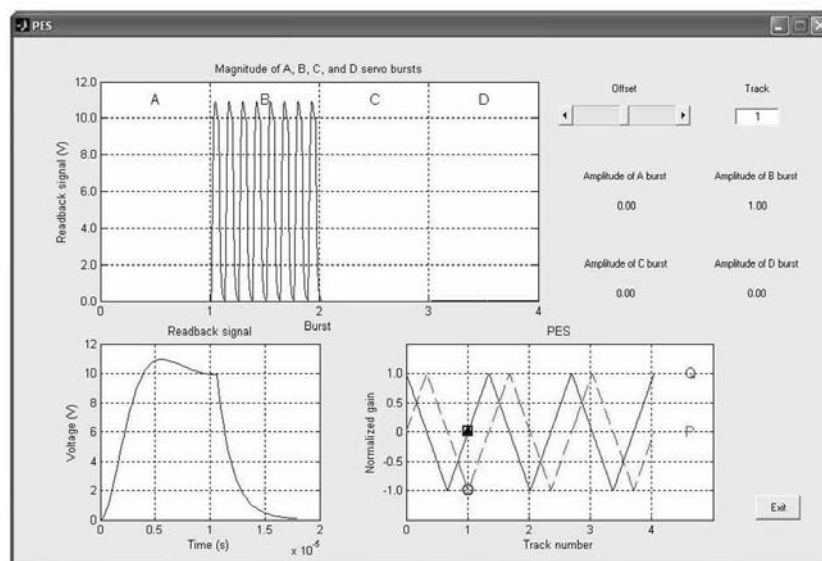


Fig. 11. MATLAB GUI for proposed PES simulation toolkit. Top: readback signal from A , B , C , and D servo bursts. Bottom-left: desired readback signal. Bottom-right: Ideal in-phase PES_P and quadrature-phase PES_Q as a function of R/W head (or probe tips) off-track.

sum of rectified C burst sampled signal

$$= \sum_{n=1}^N |\bar{C}_n|$$

sum of rectified D burst sampled signal

$$= \sum_{n=1}^N |\bar{D}_n| \quad (3)$$

where N is the predetermined number of samples. *A priori*, closed-loop control using online iterative control has been implemented successfully on this system to demonstrate the effectiveness of digital demodulation [15].

For our simulations, $N = 8$ is used and the sampling time is chosen as 18×10^{-8} s. The high sampling rate is employed for our current 'Nanodrive' setup, as the near dedicated servo PES encoding can be achieved from the usage of allocated

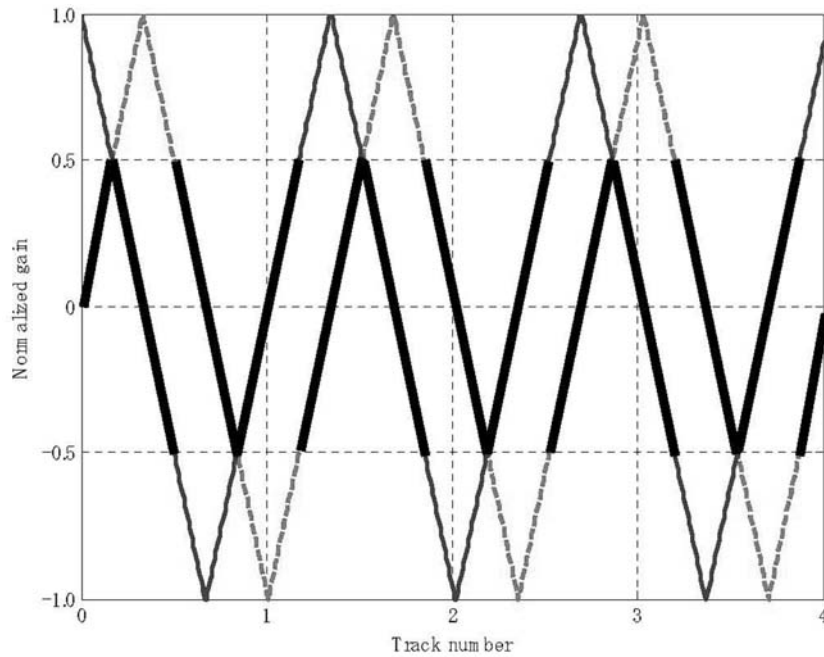


Fig. 12. Ideal in-phase PES PES_P (solid) and quadrature-phase PES PES_Q (dashed) as a function of probe tip (or R/W head) off-track. The PES (bold) is used for digital demodulation and feedback control.

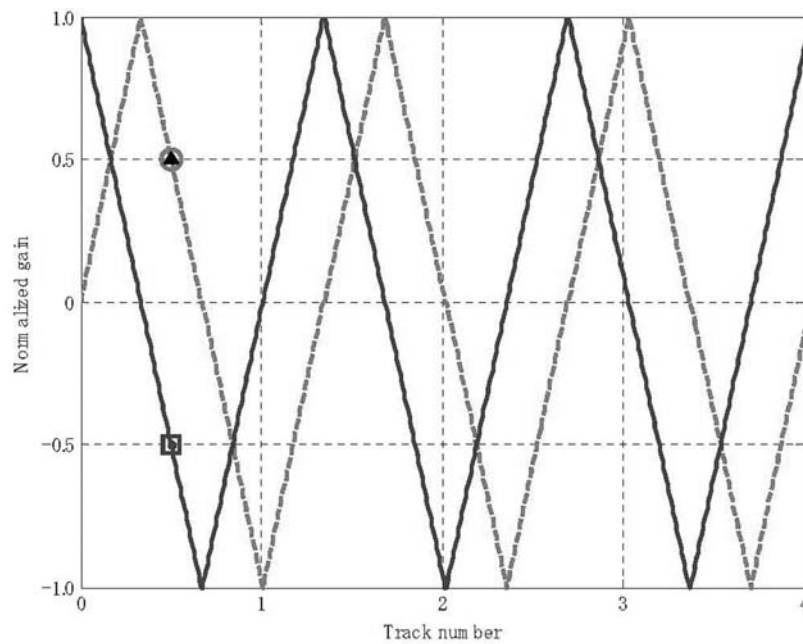


Fig. 13. Current PES p (round marker) and q (square marker) along the calibrated in-phase PES PES_P (dashed) and quadrature-phase PES PES_Q (solid), and combined PES (triangular marker) at $-1/2$ track offset from the center of Track 1.

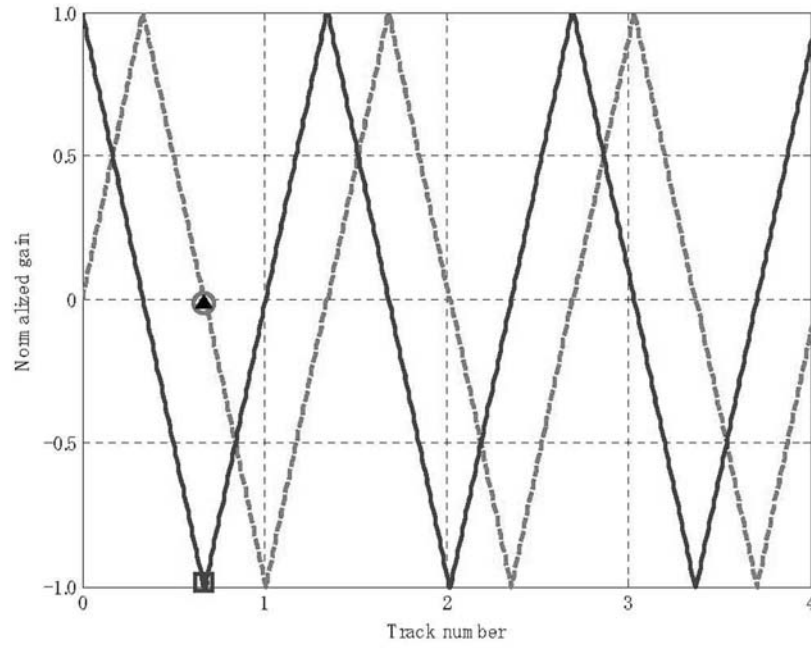


Fig. 14. Current PES p (round marker) and q (square marker) along the calibrated in-phase PES PES_P (dashed) and quadrature-phase PES PES_Q (solid), and combined PES (triangular marker) at $-1/3$ track offset from the center of Track 1

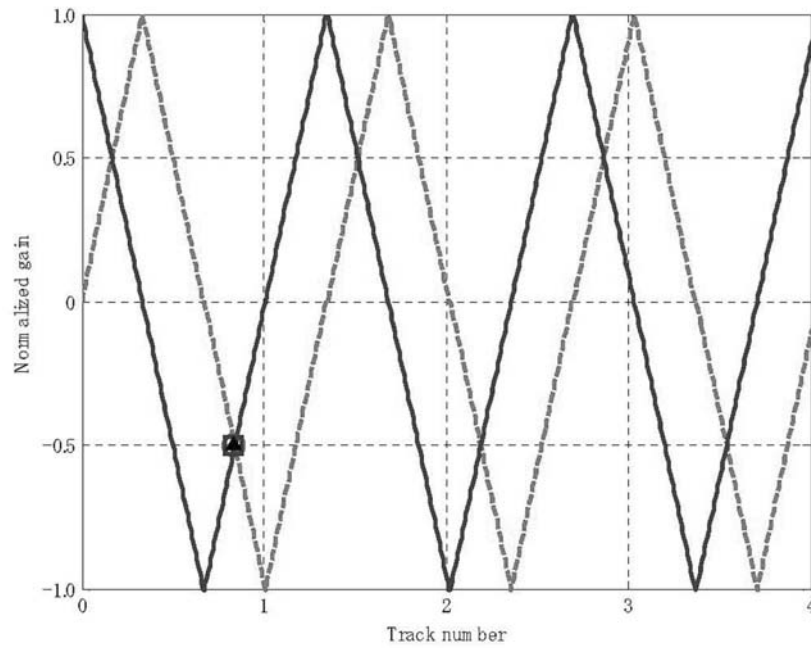


Fig. 15. Current PES p (round marker) and q (square marker) along the calibrated in-phase PES PES_P (dashed) and quadrature-phase PES PES_Q (solid), and combined PES (triangular marker) at $-1/6$ track offset from the center of Track 1.

servo fields as shown earlier in Fig. 6. Similarly, this sampling time can easily be changed in the proposed GUI as mentioned in the previous section. The sums of the magnitude for all the four servo patterns are detected. Using (3), the construction of the PES with normalization are derived as

$$\begin{aligned}
 PES_P &= \frac{1}{K} \left(\sum_{n=1}^N |\bar{A}_n| - \sum_{n=1}^N |\bar{B}_n| \right) \\
 PES_Q &= \frac{1}{K} \left(\sum_{n=1}^N |\bar{C}_n| - \sum_{n=1}^N |\bar{D}_n| \right)
 \end{aligned} \tag{4}$$

where K is the sum of readback sampled signal with unity amplitude. PES_P is known as the in-phase PES, and is zero at odd numbered tracks whereas PES_Q is known as the quadrature-phase PES and is zero at even numbered tracks. Ideally, these two derived signals should vary linearly within a track width but tends to be nonlinear in practice, especially at very high bit densities. As such, the quadrature-phase PES_Q is employed to improve linearity and reduce sensitivity to medium surface defects. Moreover, unique position decoding can be achieved with the usage of quadrature-phase PES_Q in PBSSs.

By taking the linear portions of PES_P and PES_Q , a more accurate PES can be derived from the black lines as shown in Fig. 12.

Similarly, it should be noted that only four tracks are plotted as a function of cross-track position in Fig. 12, since the PES signal is periodic with every four tracks. As such, the following relationships at an arbitrary Track N can be obtained:

- at the center of Track $4N + 1$, $[p \ q] = [-1 \ 0]$
- at the center of Track $4N + 2$, $[p \ q] = [0 \ -1]$
- at the center of Track $4N + 3$, $[p \ q] = [1 \ 0]$
- at the center of Track $4N + 4$, $[p \ q] = [0 \ 1]$

where p and q are the current PES along the calibrated in-phase PES PES_P and quadrature-phase PES PES_Q , respectively.

Illustrative examples

In this section, the perusal of the developed PES toolkit is simulated using the probe tip of PBSSs at Track 1 with offset from $-1/2$ to $+1/2$ as an example to illustrate PES linearity property. The values are

chosen in multiples of fractions of sixes as the TP is 1.5 times of the BP. In the following figures, the points in the in-phase PES PES_P (i.e. p), quadrature-phase PES PES_Q (i.e. q), and combined PES are represented by the round marker, square marker, and triangle marker, respectively.

$-1/2$ track offset

From the previous section, it had been shown that the relationship at the center of Track 1 is $[p \ q] = [-1 \ 0]$ since $N = 0$. When the slider in Fig. 11 is adjusted to the left at a track offset of $-1/2$, the value of p and q will be -0.5 and 0.5 as can be seen from the round marker and square marker in Fig. 13, respectively.

From $-1/2$ to $-1/3$ track offset, the in-phase PES PES_P is chosen as the absolute value of PES_P is less than that of PES_Q , and is shown by the triangular marker in Fig. 13 for position decoding.

$-1/3$ track offset

When the track offset is set to $-1/3$, the value of p and q will be 0 and -1 as can be seen from the round marker and square marker in Fig. 14, respectively.

From $-1/2$ to $-1/3$ track offset, the absolute value of PES_P is still less than that of PES_Q , and hence the in-phase PES PES_P shown by the triangular marker in Fig. 14 for position decoding is still employed.

$-1/6$ track offset

When track offset is set to $-1/6$, the value of p and q will both be -0.5 as can be seen from the round marker and square marker in Fig. 15.

However from $-1/6$ to the track center, the

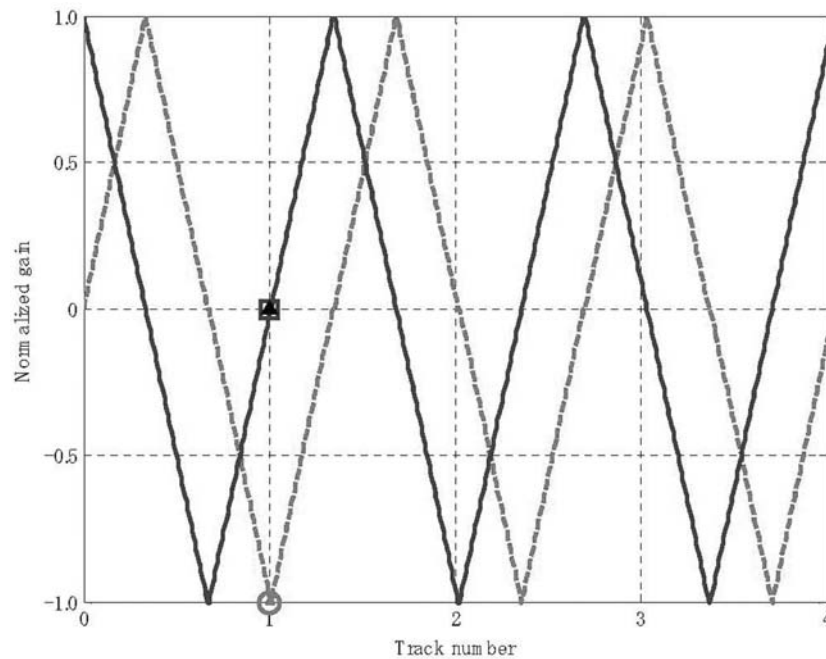


Fig. 16. Current PES p (round marker) and q (square marker) along the calibrated in-phase PES PES_P (dashed) and quadrature-phase PES PES_Q (solid), and combined PES (triangular marker) at zero track offset from the center of Track 1.

situation of PES employment for feedback control is reversed as the absolute value of PES_Q is now less than that of PES_P . As such, the quadrature-phase PES PES_Q shown by the triangular marker in Fig. 15 for position decoding will be used.

Zero track offset

At the center of the track corresponding to zero track offset, the values of p and q will both be 1

and 0 as can be seen from the round marker and square marker in Fig. 16.

At zero track offset, the probe tips (or R/W heads) are at the track center which is the ‘ideal’ position though the quadrature-phase PES PES_Q shown by the triangular marker in Fig. 14 for position decoding is used. As such, no control actions will be required since PES_Q is zero, which will keep the probe tips (or R/W heads) at

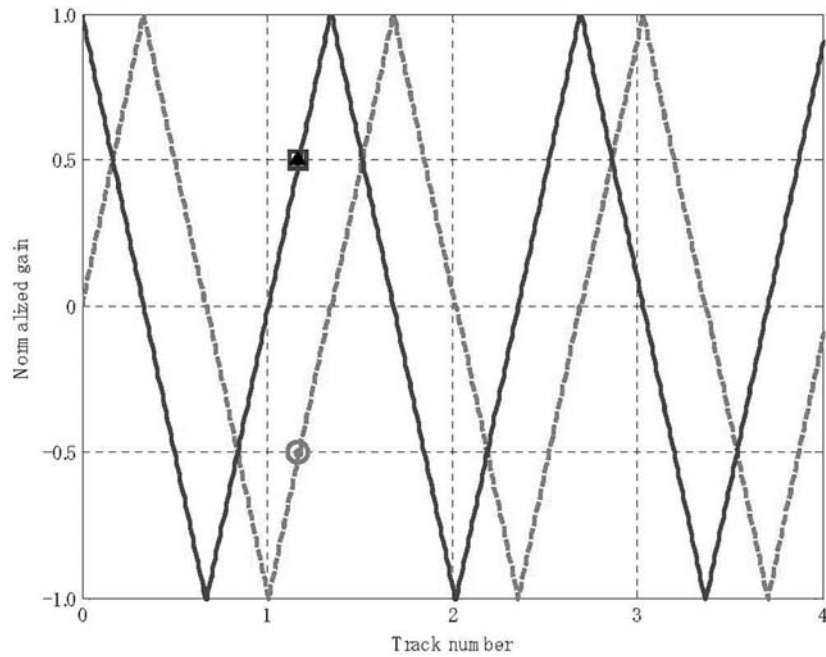


Fig. 17. Current PES p (round marker) and q (square marker) along the calibrated in-phase PES PES_P (dashed) and quadrature-phase PES PES_Q (solid), and combined PES (triangular marker) at $+1/6$ track offset from the center of Track 1.

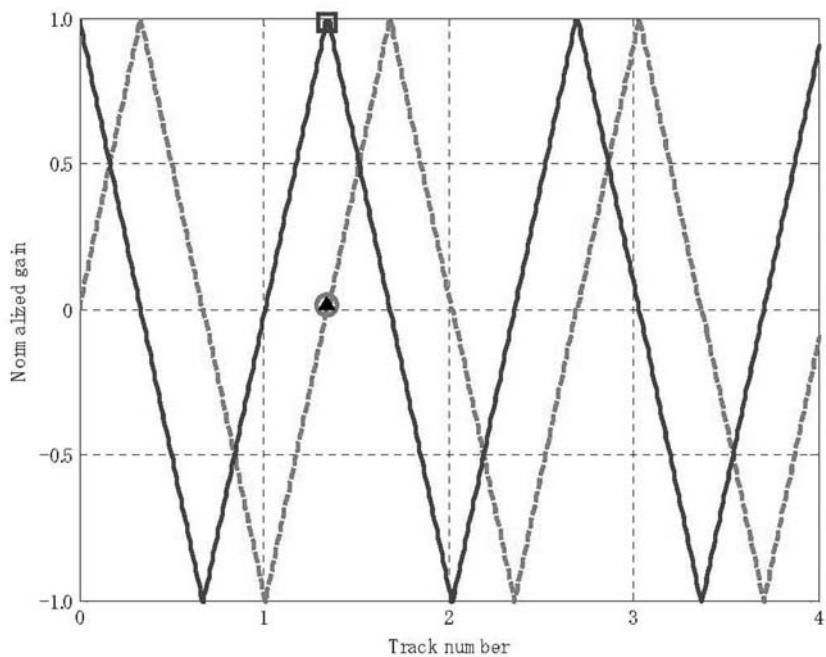


Fig. 18. Current PES p (round marker) and q (square marker) along the calibrated in-phase PES PES_P (dashed) and quadrature-phase PES PES_Q (solid), and combined PES (triangular marker) at $+1/3$ track offset from the center of Track 1.

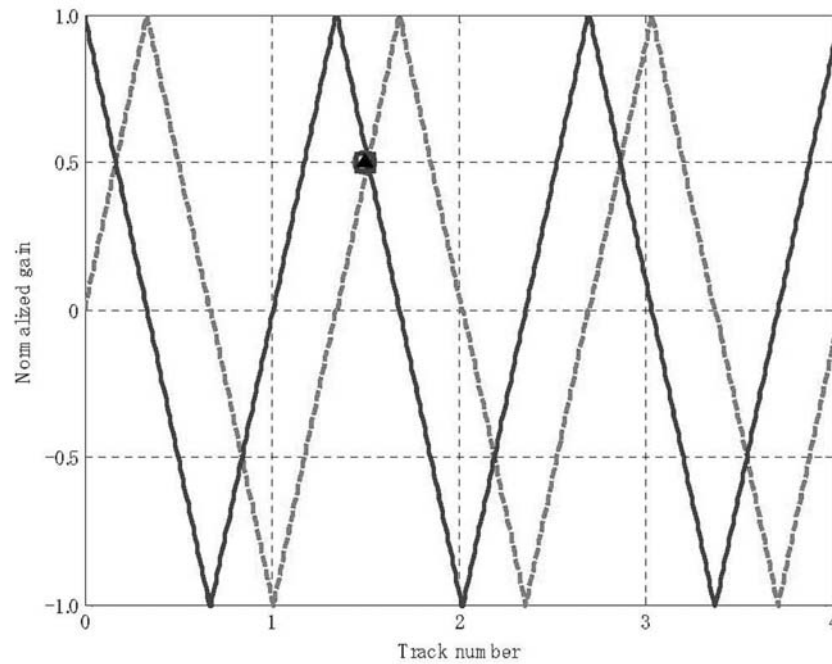


Fig. 19. Current PES p (round marker) and q (square marker) along the calibrated in-phase PES PES_p (dashed) and quadrature-phase PES PES_q (solid), and combined PES (triangular marker) at $+1/2$ track offset from the center of Track 1.

this location—corresponding to the center of the tracks—at all possible times.

For brevity but without loss of generality, the cases for the probe tips (hence R/W heads) at $+1/6$, $+1/3$, and $+1/2$ track offset are shown in Figs. 17, 18, and 19, respectively.

From the above figures, it can be clearly seen that the principle of PES decoding is identical to the cases with negative offset depicted earlier. The main essence of this decoding is that the smaller of

the absolute values of two markers is used to determine PES to ensure that R/W/E operations are executed by moving the probe tips (R/W heads) back to the track centre.

In all, the decoding scheme for a general track number N and different offsets are summarized and documented in a lookup table in Table 1. The underlined entries denote the identical value of p or q being used as the PES signal for feedback control.

Table 1. Lookup table for PES decoding scheme

Track offset	Track $4N+1$			Track $4N+2$		
	p	q	PES	p	q	PES
0	-1	<u>0</u>	<u>0</u>	<u>0</u>	-1	<u>0</u>
$-1/2 \sim -1/3$	<u>$0.5 \sim 0$</u>	$-0.5 \sim -1$	<u>$0.5 \sim 0$</u>	$0.5 \sim 1$	<u>$0.5 \sim 0$</u>	<u>$0.5 \sim 0$</u>
$-1/3 \sim -1/6$	<u>$0 \sim -0.5$</u>	$-1 \sim -0.5$	<u>$0 \sim -0.5$</u>	$1 \sim 0.5$	<u>$0 \sim -0.5$</u>	<u>$0 \sim -0.5$</u>
$-1/6 \sim 0$	$-0.5 \sim -1$	<u>$-0.5 \sim 0$</u>	<u>$-0.5 \sim 0$</u>	<u>$0.5 \sim 0$</u>	$-0.5 \sim -1$	<u>$0.5 \sim 0$</u>
$0 \sim +1/6$	$-1 \sim -0.5$	<u>$0 \sim 0.5$</u>	<u>$0 \sim 0.5$</u>	<u>$0 \sim -0.5$</u>	$-1 \sim -0.5$	<u>$0 \sim -0.5$</u>
$+1/6 \sim +1/3$	<u>$-0.5 \sim 0$</u>	$0.5 \sim 1$	<u>$-0.5 \sim 0$</u>	$-0.5 \sim -1$	<u>$-0.5 \sim 0$</u>	<u>$-0.5 \sim 0$</u>
$+1/3 \sim +1/2$	<u>$0 \sim 0.5$</u>	$1 \sim 0.5$	<u>$0 \sim 0.5$</u>	$-1 \sim -0.5$	<u>$0 \sim 0.5$</u>	<u>$0 \sim 0.5$</u>
Track offset	Track $4N+3$			Track $4N+4$		
	1	<u>0</u>	<u>0</u>	<u>0</u>	1	<u>0</u>
$-1/2 \sim -1/3$	<u>$-0.5 \sim 0$</u>	$0.5 \sim 1$	<u>$-0.5 \sim 0$</u>	$-0.5 \sim -1$	<u>$-0.5 \sim 0$</u>	<u>$-0.5 \sim 0$</u>
$-1/3 \sim -1/6$	<u>$0 \sim 0.5$</u>	$1 \sim 0.5$	<u>$0 \sim 0.5$</u>	$-1 \sim -0.5$	<u>$0 \sim 0.5$</u>	<u>$0 \sim 0.5$</u>
$-1/6 \sim 0$	<u>$0.5 \sim 1$</u>	<u>$0.5 \sim 0$</u>	<u>$0.5 \sim 0$</u>	<u>$-0.5 \sim 0$</u>	$0.5 \sim 1$	<u>$-0.5 \sim 0$</u>
$0 \sim +1/6$	$1 \sim 0.5$	<u>$0 \sim -0.5$</u>	<u>$0 \sim -0.5$</u>	<u>$0 \sim 0.5$</u>	$1 \sim 0.5$	<u>$0 \sim 0.5$</u>
$+1/6 \sim +1/3$	<u>$0.5 \sim 0$</u>	$-0.5 \sim -1$	<u>$0.5 \sim 0$</u>	$0.5 \sim 1$	<u>$0.5 \sim 0$</u>	<u>$0.5 \sim 0$</u>
$+1/3 \sim +1/2$	<u>$0 \sim -0.5$</u>	$-1 \sim -0.5$	<u>$0 \sim -0.5$</u>	$1 \sim 0.5$	<u>$0 \sim -0.5$</u>	<u>$0 \sim -0.5$</u>

CONCLUSION

In this paper, a simulation toolkit for studying PES generation in data storage system is presented. The toolkit includes a graphical user interface (GUI) developed using MATLAB. With the GUI, users of the toolkit can alter different parameters associated with the PES generation mechanism of hard disk drive and storage-based storage system. This toolkit can be used to enhance learning and understanding PES generation mechanisms of HDD and PBSS. It can also be used to analyze effects of different parameters and, therefore, to develop better PES schemes. Both students and practicing engineers can benefit from using the proposed toolkit. Simulation results show that using digital area demodulation and

the lookup table allows fast signal processing for unique position encoding to bring the probe tips or R/W heads back to the track centers effectively. Other demodulation schemes can be incorporated for comparative study between different schemes. Future works include modeling the effects of noise and disturbances on the demodulated PES, design of novel demodulation schemes, as well as creating an add-on module for a one stop digital servo controller evaluation.

The toolkit can be used to help in teaching undergraduate and graduate level courses on data storage systems. One such module, EE4506 (Magnetic Recording Systems), is offered once a year to undergraduate students of Electrical and Computer Engineering in the National University of Singapore.

REFERENCES

1. E. Eletheriou, T. Antonakopoulos, G. K. Binnig, G. Cherubini, M. Despont, A. Dholakia, U. Dürig, M. A. Lantz, H. Pozidis, H. E. Rothuizen and P. Vettiger, Millipede—A MEMS-based scanning-probe data-storage system, *IEEE Transactions on Magnetics*, **39**(2), 2003, pp. 938–945.
2. P. Vettiger and G. K. Binnig, The Nanodrive Project, *Scientific American*, **228**(1), 2003, pp. 46–53.
3. P. Vettiger, M. Despont, U. Drechsler, U. Dürig, W. Häberle, M. I. Lutwyche, H. E. Tothuisen, R. Stutz, R. Widmer and G. K. Binnig, The ‘Millipede’—more than one thousand tips for future AFM data storage, *IBM Journal of Research and Development*, **44**(3), 2000, pp. 323–340.
4. H. J. Mamin, B. D. Terris, L. S. Fan, S. Hoen, R. C. Barrett and D. Rugar, High-density data storage using proximal probe techniques, *IBM Journal of Research and Development*, **39**(6), 1995, pp. 681–700.
5. S. Singh, S. Bhatt, S. Kapoor, A. Bhavsar and B. P. Kumar, A student-accessible graphical user interface-based FDTD algorithm for visualization of electromagnetic fields, *International Journal of Engineering Education*, **21**(4), (Special Issue), 2005, pp. 625–635.
6. M. Varadarajan and S. P. Valsan, MatPECS—A MATLAB-based power electronic circuit simulation package with GUI for effective classroom teaching, *International Journal of Engineering Education*, **21**(4), (Special Issue), 2005, pp. 606–611.
7. W. E. Wong, L. Feng, Z. He, J. Liu, C. M. Kan and G. Guo, PC-based position error signal generation and servo system for a spinstand, *IEEE Transactions on Magnetics*, **41**(11), 2005, pp. 4315–4322.
8. A. H. Sacks, Position signal generation in magnetic disk drives, Ph.D. thesis, Carnegie Mellon University, (1995).
9. A. A. Mamun, T. H. Lee, G. Guo, W. E. Wong and W. Ye, Measurement of position offset in hard disk drive using dual frequency servo bursts, *IEEE Transactions on Instrumentation and Measurement*, **52**(6), December 2003, pp. 1870–1880.
10. H. Park, J. Jung, D. -K. Min, S. Kim, S. Hong and H. Shin, Scanning resistive probe microscopy: imaging ferroelectric domains, *Applied Physics Letters*, **84**(10), 2004, pp. 1734–1736.
10. L. R. Carley, J. A. Main, G. K. Fedder, D. W. Greve, D. F. Guillou, M. S. C. Lu, T. Mukherjee, S. Santhanam, L. Abelmann and S. Min, Single-chip computers with microelectromechanical systems-based magnetic memory, *Journal of Applied Physics*, **87**(9), 2000, pp. 6680–6685.
10. Y. Lu, C. K. Pang, J. Chen, H. Zhu, J. P. Yang, J. Q. Mou, G. Guo, B. M. Chen and T. H. Lee, Design, fabrication and control of a micro X–Y stage with large ultra-thin film recording media platform, *Proceedings of the 2005 IEEE/ASME International Conference on AIM*, Monterey, CA, July 24–28, 2005, MA1-04, pp. 19–24.
10. C. Li, Design and implementation of position error signals for probe-based storage systems, B.Eng. thesis, National University of Singapore, (2005).
10. A. Pantazi, M. A. Lantz, G. Cherubini, H. Pozidis and E. Eleftheriou, A servomechanism for a micro-electro-mechanical-system based scanning-probe data storage device, *Nanotechnology*, **15**(10), 2004, S612–S621.
10. C. K. Pang, W. E. Wong, G. Guo, B. M. Chen and T. H. Lee, Nonrepeatable run-out rejection using online iterative control for high-density data storage, *IEEE Transactions on Magnetics*, **43**(5), 2007, pp. 2029–2037.

Chee Khiang Pang (Justin) was born in Singapore in 1976. He received the B. Eng. (Hons.), M. Eng., and Ph. D. degrees in 2001, 2003, and 2007, respectively, all in electrical and computer engineering, from the National University of Singapore (NUS), working closely with A*STAR Data Storage Institute (DSI). In 2003, he was a Visiting Fellow in the School of Information Technology and Electrical Engineering (ITEE), University of Queensland (UQ), Brisbane, working on the probabilistic small signal stability of a large-scale

interconnected power systems project funded by Electric Power Research Institute (EPRI), Palo Alto, CA. Since 2006 he has been with Central Research Laboratory, Hitachi, Ltd., Fujisawa, Kanagawa, Japan, where he is currently a tenured researcher. In December 2007, he was a Visiting Academic in the School of ITEE, UQ, Brisbane, and was invited by IEEE Queensland Section to give a seminar. He has authored more than 20 papers in areas of HDD control and power engineering. He is a reviewer of several international refereed journals and conferences. He is an International Program Committee Member for the 2007 IEEE Congress on Evolutionary Computation (CEC). His current research interests include synergistic optimization of servo-mechanical integration, advance loop shaping for high bandwidth servos, active vibration control in mechatronics, sensor fusion for precision positioning systems, HDD single-stage and dual-stage servo systems, PBSSs, and the Self Servo-track Writing Process (SSW) process.

Wai Ee Wong was born in Singapore, and received her B.Eng. (Hons) and M.Eng. in 2001 and 2004, respectively, both in electrical and computer engineering, from National University of Singapore (NUS). Since 2003, she has been with A*STAR Data Storage Institute (DSI), Singapore, where she is currently a Senior Research Engineer. Her research interests include signal generation, simulation and experimental platform implementation, and PES generation methods in data storage channels, and servo patterning for future data storage devices.

Chengchen Li received his B.Eng. (Hons) in 2005 in electrical and computer engineering, from National University of Singapore (NUS).

Abdullah Al Mamun obtained his B.Tech. (Hons) in Electronics and Electrical Communication Engineering from IIT, Kharagpur, India, in 1985 and his Ph.D. in Electrical Engineering from National University of Singapore (NUS) in 1997. He has a range of professional experience in academia, research and industry. He is currently an Associate Professor in the department of Electrical and Computer Engineering of NUS. Prior to joining the faculty in 1999, he had various responsibilities in Maxtor (Singapore), Data Storage Institute (Singapore), and Siemens (Bangladesh) Ltd. Mamun's research interests include precision mechatronics, servomechanism in data storage devices, intelligent control and mobile robots. He has co-authored a book, *Hard Disk Drive: Mechatronics and Control*, with two colleagues from Data Storage Institute. He is the author or co-author of more than 50 articles published in premium international journals and presented at international conferences.